

A convective instability mechanism for quasistatic crack branching in a hydrogel

T. Baumberger and O. Ronsin

*INSP, UPMC Univ Paris 06, CNRS UMR 7588,
140 rue de Lourmel, 75015 Paris France*

(Dated: May 29, 2018)

Abstract

Experiments on quasistatic crack propagation in gelatin hydrogels reveal a new branching instability triggered by wetting the tip opening with a drop of aqueous solvent less viscous than the bulk one. We show that the emergence of unstable branches results from a balance between the rate of secondary crack growth and the rate of advection away from a non-linear elastic region of size \mathcal{G}/E where \mathcal{G} is the fracture energy and E the small strain Young modulus. We build a minimal, predictive model that combines mechanical characteristics of this mesoscopic region and physical features of the process zone. It accounts for the details of the stability diagram and lends support to the idea that non-linear elasticity plays a critical role in crack front instabilities.

PACS numbers: 46.50.+a, 62.20.mt

Introduction

Recent developments in tissue engineering [1] have raised polymer hydrogels to the status of genuine, *structural* materials, suitable for load bearing applications, such as scaffolds for in vivo tissue regeneration. Disregarding the biological issue, an essential step towards the rational design of such hydrogel-based systems is to understand how these “soft” solids break. This means not only relating their micro-structural features to their mechanical strength, but also describing the way failure will eventually proceed, i.e. how damage will pervade a sample set in a given mechanical as well as physico-chemical environment.

Hydrogels are network-based, solvent-swollen materials. The covalent (resp. non covalent) nature of the cross-linking bonds plays an essential role in chemical (resp. physical) gel strength. Chemical gels require C-C backbone scission to break and exhibit quasi rate-independent energy dissipation during crack propagation. Hence, fracture usually proceeds dynamically, i.e. accelerates until reaching values in the vicinity of the Rayleigh wave velocity of the material. Chemical gels are therefore termed brittle and as such have received much attention recently for their ability to mimic the dynamic fracture phenomenology of hard brittle solids, albeit at much lower velocities [2]. This is in contradistinction with physical gels in which weaker crosslinks act as mechanical fuses preventing chain scission. Disrupting large crosslink structures [3] and/or pulling chains out of the gel matrix [4] are usually strongly dissipative, rate-dependent breaking processes which are responsible for the amazing resistance to fracture of these materials, mostly consisting of solvent with only a small fraction of polymer. Steady, quasistatic crack propagation is readily achieved with physical gels. This makes them suitable for detailed investigation aimed at unraveling the physical, dissipative mechanisms at work.

Notwithstanding these fundamental differences, both physical and chemical gels have in common their softness i.e. their large elastic compliance. Consequently, the fracture process involves finite crack tip opening displacements and large deformations over a wide region ahead of the tip. This situation is markedly at odds with the requirement of linear elastic fracture mechanics (LEFM) that small strain, *linear* elasticity prevails everywhere apart from a near tip “process zone” where dissipative bond-breaking occurs. Owing to the powerful ability of LEFM to predict the onset of failure with minimal material-dependent input [5], though, the role played by the near crack-tip, non-linear elastic (NLE) zone where

LEFM breaks down, has been long overlooked. This, nevertheless, cannot be ignored any more when dealing with two important issues:

Elastic crack blunting — In soft elastic solids which can sustain bond-breaking stresses much larger than their small-strain Young modulus E , crack tips tend to blunt, i.e. to develop large radii due to purely elastic deformations [6], thereby mitigating remote stress intensification. A strict LEFM approach would lead to the paradoxical conclusion that stresses, which are predicted to plateau at values of order E , remain too low to initiate rupture [6]. Strain-hardening, a NLE characteristics shared by strongly stretched polymer networks, has been proposed as a likely way of restoring stress concentration in the near tip region.

Crack front instabilities — Smooth crack propagation, either quasistatic or dynamic, is rather the exception than the rule in fracture of soft elastic solids. Branching [2], splitting [3, 7] or oscillating [8, 9] cracks are commonly reported phenomena which LEFM fails to explain [10]. Again, the existence of the NLE zone, introducing a new length scale in the fracture problem, has been invoked as the missing ingredient for predicting the onset of a front instability and its characteristic features [11, 12]. It is worth noting that crack tip blunting and splitting have already been evoked by Gent [13] as possible *causes* of the high tear strength of visco-elastic elastomers (unswollen chemical gels). He listed them amongst several unresolved issues in rubber fracture. Indeed, despite recent advances in numerical and theoretical description of the NLE zone, elastic blunting and front instabilities remain widely open problems which probably transcend the case of hydrogels.

These materials, which feature no noticeable linear visco-elasticity over a wide frequency range, are not expected to exhibit bulk energy dissipation during crack propagation but rather localized dissipation in a near tip process zone of extension d . In the case of gelatin gels, it has been argued, based on experiments [14] that $d \sim 100$ nm. The size of the NLE zone scales with the natural length in fracture problems $\mathcal{L} = \mathcal{G}/E$ where \mathcal{G} is the energy release rate (free energy released by the advance of a unit area of crack) which, for a quasistatic crack, identifies itself with the dissipated fracture energy. In the case of gels, which are “tough” solids with relatively large \mathcal{G} and low E , \mathcal{L} ranges typically between $100 \mu\text{m}$ and a few mm (as compared, e.g. to a few Å for brittle silica glass). Thus, fracture in hydrogels exhibit a clear hierarchy of relevant length scales between the microscopic d , the mesoscopic \mathcal{L} and the macroscopic system size h :

$$d \ll \mathcal{L} \ll h$$

This configuration, which extends the so called “small scale yielding” hypothesis [16] to the NLE case, plays a central role in the following.

This article aims at presenting experimental evidence of a previously undescribed branching instability in a physical gelatin gel. The clear separation of length scales enables us to unravel NLE effects from dissipative mechanisms. The instability is therefore amenable to a physical interpretation which accounts — though schematically — for the elastic blunting of the quasistatic main crack on the scale \mathcal{L} . More precisely, the unstable onset of side branches, which we trigger by modifying dissipation locally, i.e. within the process zone itself, is proposed to result from the competition between the *growth* of secondary cracks and their *advection* in the displacement field of the main crack, out of the near tip NLE zone where opening stresses remain significant.

The article is organized as follows: in section I, the physical mechanisms of gelatin gel fracture are briefly outlined, with emphasis put on the role of solvent viscosity. The branching instability experiment is described in section II and the marginal nature of the branching onset is evidenced. This makes it possible in section III to propose a model featuring a single free parameter, lumping together the NLE properties of the blunted crack. Once this parameter is determined, the predictability of the model is successfully tested. Possible generalization of the model to other soft solids is discussed in part IV.

I. A REMINDER ON GELATIN GELS

A. Structure

Gelatin, a biopolymer made of denatured collagen, can dissolve in aqueous solvents (e.g. mixtures of water and glycerol) above the melting temperature ($T_m \simeq 40^\circ\text{C}$). Upon cooling below T_m , gelatin chains partially revert to the triple helix conformation of the native collagen, resulting in a network of rigid rods interspeded by random coils [17]. The mesh-size ξ can be evaluated from the Young elastic modulus E assuming an entropic origin for the gel elasticity: $\xi \sim (k_B T / E)^{1/3}$. It is typically on the order of 10 nm for Young moduli in the 10 kPa range.

The cross-linking triple helices are stabilized by weak physical H-bonds. Accordingly, the gel is thermoreversible. Moreover, it ages as revealed by the logarithmic increase of E with time, and exhibits slow stress relaxation typical of soft glassy materials[18]. However, on short times relevant to most fracture experiments, the polymer network can sustain shear. The relative motion of the solvent with respect to the elastic network is a collective, diffusive process with a coefficient $D_{coll} \sim E\xi^2/\eta_{bulk}$ with η_{bulk} the solvent viscosity. Typically $D_{coll} \simeq 10^{-11} \text{ m}^2.\text{s}^{-1}$, an order of magnitude which makes solvent draining a very slow process on macroscopic length scales so that, for all practical purposes, the gel samples can be considered quasi-incompressible.

Non-linear elasticity of gelatin gels exhibits strain hardening at moderate strains. As shown on figure 1, it does not obey the classical neo-hookean constitutive law [19] (corresponding to a strain energy density functional $W_{NH}(\lambda_x, \lambda_y, \lambda_z) = EJ_1/6$ with $J_1 = \lambda_x^2 + \lambda_y^2 + \lambda_z^2 - 3$ an invariant function of the principal stretch ratios, related by the incompressibility condition $\lambda_x\lambda_y\lambda_z = 1$). The data obtained in uniaxial compression are, rather, consistent with an empirical expression used in numerical fracture studies as a simple model for severe strain hardening [12]: $W_{SH} = EJ_m(\exp(J_1/J_m) - 1)/6$ with $J_m \simeq 2.3$ suggesting that for elongations of order $\sqrt{J_m + 3} \simeq 230\%$ the chains are already stretched significantly taut.

B. Fracture

Experimentally, the rate-dependent fracture energy $\mathcal{G}(V)$ for a crack propagating steadily at a markedly subsonic (or “quasistatic”) velocity V reads :

$$\mathcal{G} = \mathcal{G}_0 + \Gamma\eta_{bulk}V \quad (1)$$

with η_{bulk} the solvent viscosity, $\mathcal{G}_0 \simeq 1 \text{ J.m}^{-2}$ and $\Gamma \sim 10^6$. This linear relationship has been interpreted [4] as resulting from the fact that in this physical gel, fracture does not proceed by chain scission but rather via unzipping of the cross-links and subsequent pulling out of the overall chains to the expense of the viscous drag against the solvent. \mathcal{G}_0 stems from the plastic work for unzipping and, possibly, from the “dehydration” cost for exposing the polymer chains to air. The rate-dependent term accounts for the viscous losses against the solvent. Γ is predicted to scale as the squared ratio of the chain contour length ($\Lambda \simeq 1 \mu\text{m}$)

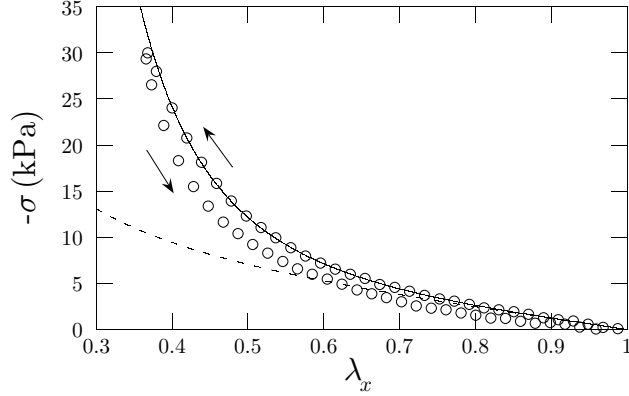


FIG. 1: Non-linear elastic response of a cylinder of gelatin gel (5 wt.% in 60%-40% glycerol-water solvent) in uniaxial compression between well lubricated plates. σ is the true (Cauchy) stress and λ_x is the compression ratio. The solid curve is a fit using a strain energy density W_{SH} (see text) with $J_m = 2.3$. The initial slope ($\lambda_x \lesssim 1$) yields the Young modulus $E = 12.1$ kPa. The dashed line corresponds to the neo-hookean elastic solid with the same small strain modulus. The small hysteresis between loading and unloading curves is probably indicative of slow stress relaxation[18] during the 6 s duration of the cycle.

to the mesh size of the network ($\xi \simeq 10$ nm).

Note that the stress level at the crack tip, given by \mathcal{G}/Λ is always several order of magnitude larger than the Young modulus. This is precisely the case where elastic blunting of the crack is predicted, hence where a marked NLE zone ahead of the crack tip is expected [6].

The sensitivity of the fracture energy to solvent viscosity makes it possible to estimate the extension d of the process zone where energy is dissipated [4]. This is achieved by wetting the crack tip opening with a drop of solvent of viscosity $\eta_{\text{drop}} < \eta_{\text{bulk}}$. Both drop and bulk solvents differ only by their fractions of glycerol in water which tend to equilibrate via molecular diffusion, with a coefficient D_{gly} . Experimentally, the drop acts as a reservoir. The glycerol content of the gel ahead of the moving tip adjusts from the drop concentration to the bulk one over the diffusive skin depth of order D_{gly}/V . At low enough velocities, the effective viscosity

$$\eta_{\text{eff}} = \Gamma^{-1} \frac{d\mathcal{G}}{dV} \quad (2)$$

which accounts for the advance of “rinsing” within the process zone is that of the drop liquid. As V increases above $V_{\text{diff}} \simeq D_{\text{gly}}/d$, $\eta_{\text{eff}}(V)$ gradually grows up to η_{bulk} . Measuring

V_{diff} yields $d \simeq 100$ nm.

This estimate was obtained originally [4] with a relatively small viscosity contrast, $\eta_{\text{bulk}}/\eta_{\text{drop}} \simeq 3$. Unexpectedly, on attempting to reproduce the experiment with a larger contrast, a spectacular branching instability was observed. It is the aim of this paper to describe and interpret this phenomenon.

II. EXPERIMENTAL

A. Material and methods

Gel samples are composed of 5 wt.% of gelatin (Sigma, “300 Bloom” grade) in aqueous solvents containing from $\phi = 0$ to 70 wt.% of glycerol in water. The pregel solution is prepared by letting gelatin dissolve in its solvent at 85°C under gentle stirring. It is poured into rectangular molds (length $L = 300$ mm, width $h = 30$ mm, and thickness $e = 10$ mm) and “set” at 5°C for 10 hours. Before performing any experiment, the samples are left to equilibrate at room temperature ($T \simeq 20^\circ\text{C}$) for 2 hours. Aging during the duration of an experimental run (about 2 min) has been checked to be negligible. The samples are characterized by their small strain Young moduli E (between 9 and 15 kPa, increasing with glycerol content) and their solvent viscosity η_{bulk} (from 1 cP for pure water to 22 cP at $\phi = 70\%$).

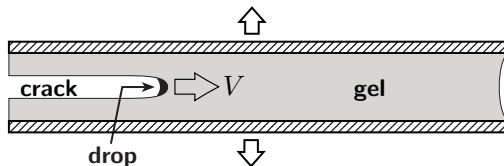


FIG. 2: Schematic experimental setup. The gel sample is stretched between two rigid, parallel grips so that the energy release rate is imposed. The steady-state crack front velocity V is measured.

Wetted crack experiments are performed with a setup fully described elsewhere [14]. Gel plates are stretched along their width by imposing a displacement Δh to the rigid grips (see Fig.2). Due to the large aspect ratio $L/h = 10$, uniform stretching is realized in a significant portion of the sample, thereby storing a prescribed amount of elastic energy \mathcal{G} to be ultimately released per unit area of a straight crack propagating along the length. $\mathcal{G}(\Delta h)$

is evaluated as $\mathcal{W}/(eL)$ with \mathcal{W} the measured work required to stretch an un-notched sample by Δh . Note that, although the expression for \mathcal{G} is strictly valid for infinitely long samples [15], it is expected to provide a reasonable approximation to within about $h/L = 10^{-1}$. The loading rate for the calibration test is chosen high enough for stress relaxation to be negligible during the load (see eg. Fig 1). Also the phenomenon reported in the present study occurs on time scales short enough for internal dissipation associated with remote stress relaxation to be negligible in comparison with the energy released by the fracture itself.

Crack propagation is initiated by cutting a notch at one end of the plate. Away from the sample edges, when the crack velocity reaches a steady value V of order a few mm.s^{-1} , a drop ($\simeq 200 \mu\text{L}$) of a water/glycerol mixture of viscosity η_{drop} is quickly injected into the tip opening where it remains trapped by capillarity and gravity (the crack travels downward vertically). The subsequent dynamics of the crack tip is monitored at 10 frames per second by a video camera mounted on a traveling stage so as to keep the crack front within the field of view.

B. Characteristics of the branching instability

Figure 3 shows the first stage of the instability triggered by pure water ($\eta_{\text{drop}} = 1 \text{ cP}$) wetting the tip of a gel with $\phi = 60\%$ ($\eta_{\text{bulk}} = 11 \text{ cP}$). Within a few seconds, the gel ahead of the crack is pervaded by a 3D damaged zone made of microcracks. The zone coarsens until the average front becomes flat. At that point, the fracture process is almost inhibited (for the subsequent slow return to a straight, dry crack, see movie [20]).

This spectacular, bursting response to a rather modest environmental change is in marked contrast to our previous report [14] on the wetting by pure water of a $\phi = 30\%$ gel ($\eta_{\text{bulk}} = 1.8 \text{ cP}$). Then, while being markedly accelerated the crack remained straight. Crack acceleration was ascribed to two solvent effects: firstly, wetting the tip prevents the extracted chains from being exposed to air, hence a significant lowering of the threshold energy \mathcal{G}_0 ; secondly, the water drop induces an osmotic imbalance, hence a glycerol depletion ahead of the tip, as described in I.B. Both effects contribute to cutting down the fracture energy. Since the energy release rate is imposed, it results in the observed speeding up of the crack. Fig.3 shows that, beyond this effect, local solvent dilution can destabilize a crack tip as well,

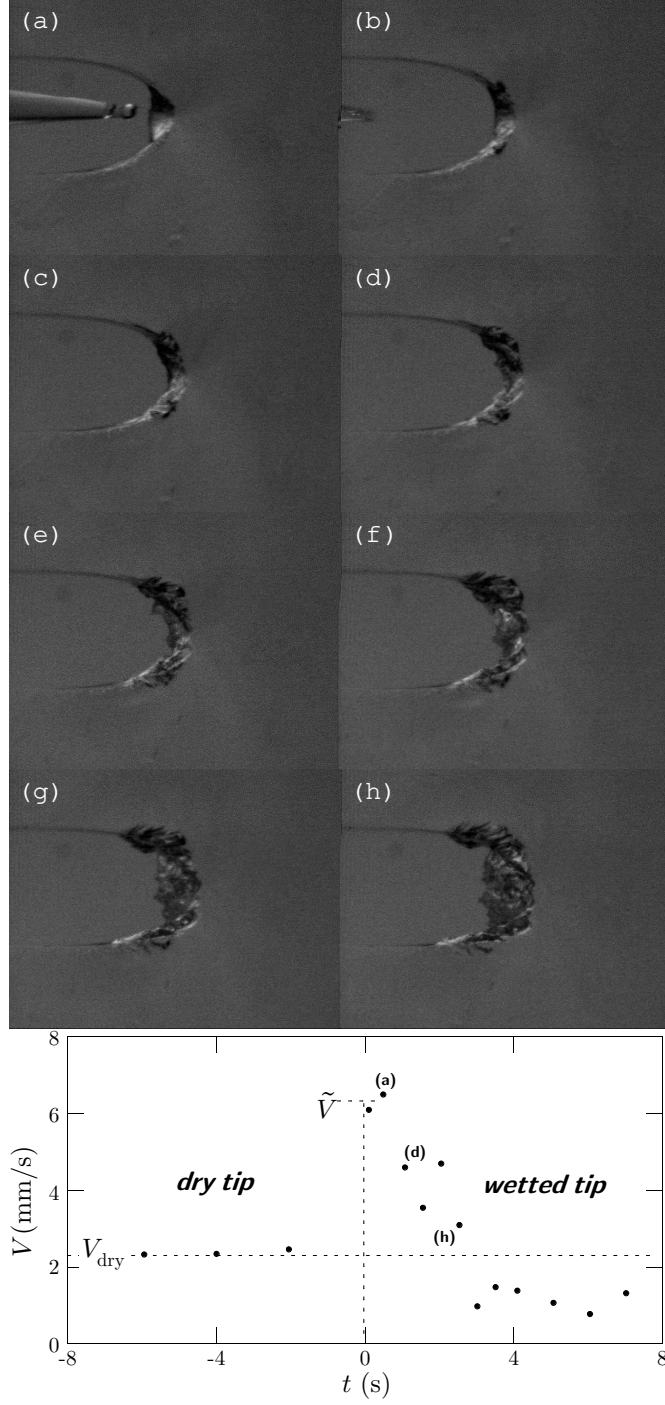


FIG. 3: Snapshots ($\Delta t = 0.3$ s) extracted from a movie [20] showing the coarsening of a microcracked zone ahead of a crack tip wetted at $t = 0$ by a drop of pure water in a $\phi = 60\%$ gel. Crack tip opening is 12 mm ($\mathcal{G} = 65$ J.m $^{-2}$). The graph displays the front velocity before and after tip wetting.

depending on the bulk viscosity.

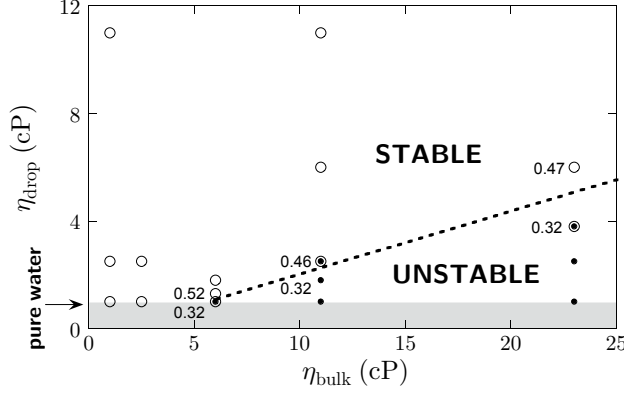


FIG. 4: Stability diagram at constant crack tip opening (12 mm) for cracks in gels with bulk water/glycerol solvents of viscosities η_{bulk} wetted by drops of viscosities η_{drop} . The shaded zone is out of experimental reach. Near critical data are labeled by the values of the compound parameter $(\eta_d/\eta_{\text{bulk}}) \cdot (\tilde{V}/V_{\text{dry}})$ with \tilde{V} and V_{dry} defined on Fig.3. The dashed line is the *predicted* locus of critical cracks (see text, section IIID).

In order to clarify this point we have mapped the stability of the crack onto the $(\eta_{\text{bulk}}, \eta_{\text{drop}})$ plane for a prescribed 12 mm crack tip opening. As displayed on Fig.4, branching occurs for large enough viscosity contrasts. Since the tip solvent cannot be made more inviscid than pure water, there is a minimal bulk viscosity, corresponding to $\phi = 50\%$ below which the crack remains stable whatever the tip environment. Fig.5 shows a snapshot of a crack in this marginal gel ($\phi = 50\%$), 4.8 seconds after being wetted by a drop of pure water. Though no thick damaged zone develops ahead of the tip, the crack path exhibits distinct undulations and aborted side branches. Moreover, before these secondary cracks stopped, they started themselves to branch, which we interpret as an interrupted cascading process that, if unimpeded, would have led to the microcracked zone of Fig.3

Now, for a gel with a bulk viscosity above the marginal one, increasing the drop viscosity from that of pure water changes the state of crack propagation from the unstable one shown on Fig.3 to a stable one via a regime similar to that described above (see movies[20]). It is therefore legitimate to term “critical” this regime of crack emission which marks systematically the frontier between stable and unstable fracture.

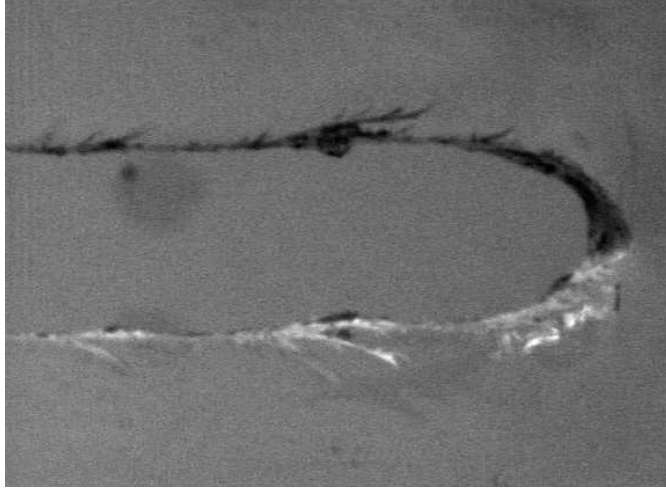


FIG. 5: Wet crack in a critical state exhibiting aborted side branches.

III. A SCHEMATIC MODEL

Disregarding the complex, fully developed structure of Fig.3, we now focus on the critical regime and propose a criterion for the onset of instability that combines the microscopic model of fracture energy specific for physical hydrogels such as gelatin and the more generic concept of a mesoscopic near-tip, non-linear elastic (NLE) zone. As a starting point we note that secondary cracks are emitted in the close vicinity of the main tip. While they grow, they are progressively advected away and gradually close on approaching the straight, traction free crack edges. Thus, there is a competition between growth and advection rates. We propose that only those cracks which manage to grow significantly before being advected out of the near-tip zone, where opening stresses are significant, can in turn branch, hence trigger a cascading process. We therefore describe branching as a *convective* instability[24].

A. Near-tip stress field of a blunted crack

Branching requires nucleation and growth of secondary cracks which eventually compete with the initial main crack to release elastic energy. We assume in the following that nucleation sites, or flaws, are provided by the inhomogeneities — of either toughness or stiffness — of the randomly crosslinked polymer network.

As a consequence of elastic blunting, associated to strain-hardening of the gel, the region where opening stresses are high is along the crack face rather than directly ahead of the

crack tip, a qualitative feature which is clearly revealed by finite element simulations [12]. This suggests that branching probably originates from nucleation and growth of edge cracks in this quasi-uniaxially stressed zone. Its extension is provided, in a first approximation, by the radius of curvature of the near tip parabolic crack opening. This is given, within a multiplicative constant of order unity, by \mathcal{G}/E . This classical result of LEFM [5] remains valid in the NLE case, at least for a neo-hookean solid (see e.g. [12]), and is certainly dimensionally correct for more strongly strain hardening materials.

We now aim at writing a growth equation for an edge crack in the NLE stress field. This is a desperately complex mechanical problem. We therefore make one further step and, based on the previously described structure of the near-tip stress field [12], we schematize the blunted elastic zone as a strip of size $\sim \mathcal{G}/E$, uniformly stretched by a stress σ_0 perpendicular to the fracture plane (see Fig.6). The material is assumed to have strain-hardened up to a state characterized by a uniform small strain modulus $E_{\text{eff}} > E$.

Progressive building-up of strain hardening on approaching the blunted crack tip is now replaced by a stepwise jump in small strain modulus at a distance \mathcal{G}/E . The unknown stress σ_0 is determined according to the compatibility requirement that LEFM should hold in the outer region. There, the stress intensity factor [5] $K_I \sim \sqrt{\mathcal{G}E}$, hence the stress at a distance \mathcal{G}/E is $\sigma_0 \sim K_I/\sqrt{\mathcal{G}/E} \sim E$. Note that this rough schematization of the blunted elastic zone is akin to that proposed in [6] on the basis of slightly different arguments.

B. Growth mechanism for a secondary crack

Since we are interested in the onset of unstable branches, we assume the length ℓ of the secondary crack to remain small as compared to the extension \mathcal{G}/E of the blunted crack zone, so that it can be treated as an edge crack which does not interfere significantly with the stress field of the main crack. For the sake of simplicity, we estimate the corresponding energy release rate $\mathcal{G}_{\text{branch}}$ according to LEFM [5] in a material with an effective Young modulus E_{eff} . Within a factor of order unity: $\mathcal{G}_{\text{branch}} = (\pi\sigma_0^2/E_{\text{eff}})\ell = \beta E\ell$, where we have introduced a dimensionless factor $\beta \approx E/E_{\text{eff}}$ which is indicative of the level of strain-hardening. The clear separation of lengthscales, $d \ll \mathcal{G}/E$, makes it legitimate to assume that the edge crack dynamics on scale \mathcal{G}/E is ruled by the same physical mechanism as the main crack. The growth equation is thus obtained by equating $\mathcal{G}_{\text{branch}}$ with the fracture energy \mathcal{G} given by

(1), replacing V by $d\ell/dt$:

$$\beta E \ell = \mathcal{G}_0 + \Gamma \eta_{\text{branch}} \frac{d\ell}{dt} \quad (3)$$

where η_{branch} is the effective solvent viscosity “felt” by the chains pulled out of the process zone ahead of the secondary crack.

As discussed in the following section, a possible rate-dependence of η_{branch} can be ruled out. Solving eq. (4) for $\ell(t)$ is therefore straightforward : $\ell(t) = \ell_c + (\ell_0 - \ell_c) \exp(t/\tau)$. Accordingly, any supercritical seed crack of initial size $\ell_0 > \ell_c = \mathcal{G}_0/\beta E$ will grow exponentially over a characteristic time

$$\tau = \frac{\Gamma}{\beta} \frac{\eta_{\text{branch}}}{E} \quad (4)$$

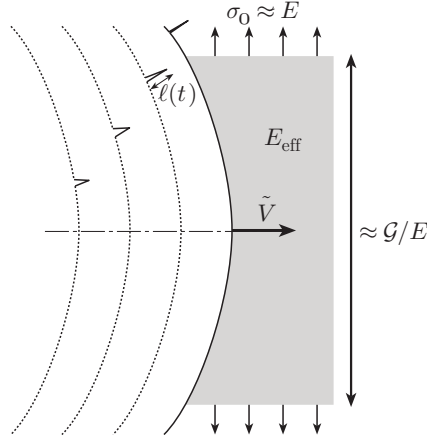


FIG. 6: Schematic representation of a secondary crack growth and advection in the NLE zone of a blunted main crack.

If the secondary crack is left to grow in the constant stress field it will eventually, at times on the order of τ , compete with the main crack for releasing energy, and give rise, in turn, to side branches. However, while the main crack grows, the root of the secondary crack is advected away from the main tip, eventually leaving the NLE zone where sufficient stress exists to permit branch growth. The stability criterion discussed in the following is based on the competition between these two effects.

C. A criterion for stable, wetted cracks

The life time of a secondary crack is given by the duration of its travel along the blunted tip zone as it is advected away from the apex of the main crack. An upper value for this duration is the time required for crossing a region of size \mathcal{G}/E at \tilde{V} , the velocity of the main crack tip in its wetted state :

$$T_{\text{adv}} = \frac{1}{\tilde{V}} \frac{\mathcal{G}}{E} \quad (5)$$

As long as $\tau > T_{\text{adv}}$, all secondary cracks will stay in their embryonic states and never compete with the main crack which will therefore remain stable. Since, according to (2), \tilde{V} is given implicitly for a prescribed \mathcal{G} by

$$\mathcal{G} = \mathcal{G}_0 + \Gamma \eta_{\text{eff}}(\tilde{V}) \tilde{V} \quad (6)$$

with \mathcal{G}_0 being usually negligible (see Fig.7), the stability criterion reads: $\eta_{\text{branch}}/\eta_{\text{eff}}(\tilde{V}) > \beta$.

At this stage, it is crucial to realize that the dynamics of the secondary crack is ruled by the effective viscosity η_{branch} which depends on glycerol diffusion, i.e. on the velocity of the branch tip with respect to the liquid drop. Since the latter is driven by capillarity and gravity along with the main crack, the relevant velocity is that at which the secondary tip cuts into the primary crack lips, i.e. $d\ell/dt$. We have therefore $\eta_{\text{branch}} = \eta_{\text{eff}}(d\ell/dt)$. Since $d\ell/dt$ remains much smaller than the velocity \tilde{V} of the main tip during the maturation phase (secondary crack growth times $t < \tau$), one can expect that $\eta_{\text{eff}}(d\ell/dt) < \eta_{\text{eff}}(\tilde{V})$. In fact, it can be shown that $\eta_{\text{branch}} = \eta_{\text{drop}}$ (see appendix) so that, finally, the criterion for a crack to remain *stable* at a quasistatic velocity \tilde{V} reads simply:

$$\frac{\eta_{\text{drop}}}{\eta_{\text{eff}}(\tilde{V})} > \beta \quad (7)$$

D. Experimental tests of the model

The above stability criterion (7), is expressed in terms of the effective viscosity functional, defined by (2), and parameter β . The former accounts for the local modification of the microscopic process zone via solute diffusion, the latter is aimed at catching the NLE modification of the gel at the mesoscopic scale of the blunted crack opening.

Let us note in the first place that, in the destabilizing configuration where the drop is less viscid than the bulk solvent, the inequality \tilde{V} : $\eta_{\text{drop}}/\eta_{\text{eff}}(\tilde{V}) \leq 1$ holds for any combinations

of \tilde{V} , η_{drop} and η_{bulk} , including those corresponding to stable cracks. Hence, according to (7), $\beta < 1$. So, in spite of the numerous multiplicative constants of order unity hidden in β , this parameter therefore retains its physical flavour as a qualitative indicator of the level of strain hardening : $\beta \sim E/E_{\text{eff}} < 1$.

Furthermore, since η_{eff} is an increasing function of the tip velocity, (7) predicts that cracks are stable at low enough velocities. This is a counter intuitive result, owing to the proposed convective nature of the instability, since for a slow main crack, side branches are only slowly advected away from the tip zone, hence have *a priori* more time to grow. The fact that this direct effect of \tilde{V} disappears in (7) can be traced back to the V -dependence of the NLE length scale $\mathcal{G}(V)/E$. A slow crack offers a shorter NLE zone for branches to grow. The existence of a lower critical velocity for a given pair $\eta_{\text{drop}} < \eta_{\text{bulk}}$ is therefore a strong test of the validity of our schematic model. We have checked it by increasing stepwise the crack opening, hence \mathcal{G} , while keeping the tip wet by continuous solvent dripping. Fig.7 shows the results for a pure water drop wetting a $\phi = 60\%$ gel. Indeed, the crack remains stable as long as $\tilde{V} < \tilde{V}_c$ with $\tilde{V}_c \simeq 4.7 \text{ mm.s}^{-1}$.

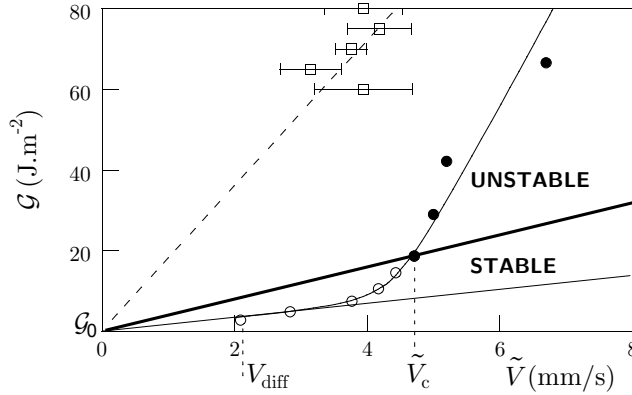


FIG. 7: Stability diagram in the fracture energy *vs.* crack-tip velocity plane. Unwetted (\square) cracks; stable (\circ) and unstable (\bullet) cracks wetted by pure water (for unstable cracks, \tilde{V} is the front velocity measured just after wetting, see Fig.3). The curve is a guide for the eyes. Slopes of the thin, thick and dashed lines are in the ratio $\eta_{\text{tip}} : \eta_{\text{eff}}(\tilde{V}_c) : \eta_{\text{bulk}}$. V_{diff} and \tilde{V}_c are defined in the text.

This enables us to evaluate β quantitatively. Following the above discussion, for $\tilde{V} < V_{\text{diff}}$ the tip is fully rinsed and $\eta_{\text{eff}} \simeq \eta_{\text{drop}}$, hence $\mathcal{G} \sim \eta_{\text{drop}} \Gamma \tilde{V}$. Fitting the low velocity data accordingly yields $\Gamma \simeq 1.6 \times 10^6$, a value compatible with that of non-wetted cracks in a companion sample of the same gel (see Fig. 7). At the critical point, we measure $\eta_{\text{eff}}(\tilde{V}_c) =$

$(\mathcal{G}(\tilde{V}_c) - \mathcal{G}_0)/(\Gamma\tilde{V}_c)$ from which we deduce that $\beta \simeq 0.42$.

Finally, we return to the stability diagram of Fig.4. Though chosen for the sake of its experimental simplicity, the constant crack tip opening prescription is theoretically awkward since it corresponds to a non trivial section of the critical surface in the 3D control parameter space $(\eta_{\text{bulk}}, \eta_{\text{drop}}, \tilde{V})$. It is nevertheless possible to make use of this diagram for an independent check of the model by recasting criterion (7) in terms of V_{dry} (resp. \tilde{V}), the crack velocities before (resp. just after) tip wetting (see Fig.3). Neglecting \mathcal{G}_0 , the constant opening imposes $\mathcal{G} \simeq \eta_{\text{bulk}}\Gamma V_{\text{dry}} \simeq \eta_{\text{eff}}(\tilde{V})\Gamma\tilde{V}$, hence the stability condition : $(\eta_{\text{drop}}/\eta_{\text{bulk}}) \cdot (\tilde{V}/V_{\text{dry}}) > \beta$. We have computed the left hand side compound parameter for near critical data on both sides of the bifurcation (see Fig.4). Remarkably, the figures systematically bracket the value $\beta = 0.42$ determined from the critical velocity.

IV. CONCLUDING REMARKS

We have identified and analyzed a new branching instability occurring in the tip vicinity of a quasistatic crack in gelatin hydrogels. We have proposed what we think is the first predictive model of a *convective* crack branching instability in a disordered elastic material. The key ingredient is the existence of a mesoscopic zone ahead of the crack where residual opening stresses are large enough for promoting side branching. The finite size of this near tip zone, which scales with \mathcal{G}/E , results in a finite advection time of incipient branches away from the main crack. Whether catastrophic crack growth occurs during this time chiefly depends on the rate-dependence of the fracture energy. In the case of gelatin, it can be conveniently tailored by a local “osmotic” control of the process zone.

Beyond the deciphering of a puzzling phenomenon which might, at first sight, appear as an idiosyncrasy of gelatin gels, we think that our analysis lends support to the emerging idea that the non-linear elastic field which bridges between the process zone and the generic linear elastic region, plays a crucial role in crack dynamics and, more specifically, in crack front instabilities [22]. Though branching instabilities have been mostly documented for fast cracks, our study indicates that they could prevail as well for slow ones over wide domains of their mechanical control parameters (crack tip velocity, tip environment, structural disorder, ...).

To go one step further along this line, let us analyze a case where quasistatic crack

propagation would be ruled by a fracture energy that depends as a sublinear power-law on the crack velocity, say:

$$\mathcal{G} = \mathcal{G}_0[1 + (V/V_0)^\alpha] \text{ with } \alpha < 1$$

Such a functional form is typical of elastomers [13] and has been reported for gels made of solvated triblock copolymers as well [3]. In the case of elastomers, the material-dependent reference velocity V_0 depends on temperature, presumably via the visco-elastic spectrum of the material. We assume that the generalized small-scale yielding approximation ($d \ll \mathcal{G}/E \ll L$) holds here.

The growth equation $\mathcal{G}(\dot{\ell}) = \beta E \ell$ for an edge crack nucleated within the primary blunted tip region can be solved analytically. It is straightforward to establish that the degree of supercriticality of the crack, introduced for the sake of simplicity as $\epsilon(t) = \ell(t)/\ell_c - 1$ with $\ell_c = \mathcal{G}_0/\beta E$, reads:

$$\epsilon(t) = \frac{\epsilon_0}{(1 - t/\tau')^{1/\gamma}} \text{ with } \tau' = \frac{\ell_c}{V_0 \gamma \epsilon_0^\gamma} \text{ and } \gamma = \alpha^{-1} - 1 > 0$$

Crack length divergence at finite time τ' signals an instability. It is important to note, however, that the time τ' for catastrophic failure depends on $\epsilon_0 = \epsilon(0)$, the initial degree of supercriticality of the unstable crack seed.

Due to advection of the material in the tip region, the main crack will however remain stable against side branching provided that $V\tau' > \mathcal{G}(V)/E$, i.e.

$$\frac{V/V_0}{1 + (V/V_0)^\alpha} > \beta \gamma \epsilon_0^\gamma \quad (8)$$

Here, in contradistinction with the $\alpha = 1$ case, a secondary crack will close back before exploding if the main one is driven at a *high* enough velocity (the rhs of (8) is an increasing function of V/V_0). Yet, this upper critical velocity depends on the strength ϵ_0 of the nucleation seed. The larger the flaw, the more destabilizing it is for the main crack. Such an instability would possibly manifest itself as follows: in the absence of any external triggering, a crack running steadily at a velocity V would eventually become unstable, provided it meets a flaw of sufficient strength. Since, according to (8), the size of the critical seed increases with V , the higher the velocity, the lower the probability of meeting such a nucleation site and the longer, statistically, the crack would remain stable.

This example shows that, even in its simplest version, our model predicts a wealth of qualitative behaviors. It prompts us to have a fresh look at the complex, intermittent dynamics reported in the case of triblock copolymer gels [3], and still unexplained. It also points to the important role played by the structural disorder on branching and suggests to study controlled, inhomogeneous materials such as filled elastomers or bicomponent, phase-separated polymer hydrogels.

Appendix

In this appendix, we show that the velocity of a branch is, in its maturing phase, small enough so that its process zone is fully rinsed by the drop i.e. that $\eta_{\text{branch}} = \eta_{\text{drop}}$ holds in eq. 4.

Consider a supercritical crack seed of initial length $\ell(0) = (1 + \epsilon_0)\ell_c$. For $t < \tau$, the crack velocity remains close to its initial value $v_0 = \epsilon_0\ell_c/\tau = \epsilon_0\mathcal{G}_0/(\eta_{\text{branch}}\Gamma)$. Since $\eta_{\text{branch}} \geq \eta_{\text{drop}} \geq \eta_{\text{water}}$, and $\mathcal{G}_0 \simeq 1 \text{ J.m}^{-2}$, $v_0 < \epsilon_0 \times 1 \text{ mm.s}^{-1}$. We argue in the following that, in our experiments, ϵ_0 remains small enough so that $v_0 < V_{\text{diff}}$.

Our model assumes that “flaws” preexist in the sample and act as edge crack seeds when reached by the blunted tip zone of the main crack. As already mentioned, flaws are ascribed to frozen fluctuations of the polymer network structure [23], e.g. via its crosslink density. Such inhomogeneities remain after coarse-graining up to the scale d of the process zone and result in a spatially modulated gel strength about an average value $\bar{\mathcal{G}}_0$, as evidenced by the roughness of fracture surfaces in gelatin gels [7]. An estimate of the maximum amplitude of \mathcal{G}_0 variations, $\Delta\mathcal{G}_0/\bar{\mathcal{G}}_0 \simeq 14\%$, has been obtained by analyzing the pinning of very slow crack fronts induced by “tough” spots [7].

According to Griffith’s theory [5], crack initiation results from a balance between the fracture energy cost \mathcal{G}_0 and the elastic energy released in a deformed region scaling with ℓ . That is a nucleation process, with an activation energy corresponding to a critical crack length ℓ_c . With $\bar{\mathcal{G}}_0 \simeq 1 \text{ J.m}^{-2}$, $\ell_c = \bar{\mathcal{G}}_0/\beta E \simeq 100 \mu\text{m}$. The activation barrier $\mathcal{E}_{\text{act}} \sim \bar{\mathcal{G}}_0\ell_c e$, with e the lateral extension of the crack, is always orders of magnitude larger than $k_B T$ whence thermal activation cannot be responsible for the distribution of initial crack lengths. We propose here that it rather reflects the statistical distribution of the flaw strengths \mathcal{G}_0 , at the scale of d and therefore identify the supercriticality index ϵ_0 with $\Delta\mathcal{G}_0/\bar{\mathcal{G}}_0$ so that

$v_0 < 1 \text{ mm.s}^{-1}$. With $D_{\text{gly}}(\phi = 60\%) = 2 \times 10^{-10} \text{ m}^2.\text{s}^{-1}$ and $d \simeq 100 \text{ nm}$, $V_{\text{diff}} \simeq 2 \text{ mm.s}^{-1}$. Since $v_0 < V_{\text{diff}}$, one may therefore safely consider that $\eta_{\text{branch}} \simeq \eta_{\text{eff}}(v_0) \simeq \eta_{\text{drop}}$.

Acknowledgments

We thank Christiane Caroli for constructive criticism and careful reading of the manuscript, and David Martina for his serendipitous discovery of the instability.

-
- [1] J. L. Drury and D. J. Mooney, *Biomaterials* **24**, 4437 (2003).
 - [2] A. Livne, G. Cohen, and J. Fineberg, *Phys. Rev. Lett.* **94**, 224301 (2005).
 - [3] M. E. Seitz, D. Martina, T. Baumberger, V. R. Krishnan, C.-Y. Hui, and K. R. Shull, *Soft Matter* **5**, 447 (2009).
 - [4] T. Baumberger, C. Caroli, D. Martina, *Nature Materials*, **5**, 552 (2006).
 - [5] B. Lawn, *Fracture of Brittle Solids*, 2nd Ed. (Cambridge, The University Press, 1993).
 - [6] C.-Y. Hui, A. Jagota, S. J. Bennison, and J. D. Londono, *Proc. Roy. Soc. London A* **459**, 1489 (2003).
 - [7] T. Baumberger, C. Caroli, D. Martina, and O. Ronsin, *Phys. Rev. Lett.* **100**, 178803 (2008).
 - [8] A. Livne, O. Ben-David, and J. Fineberg, *Phys. Rev. Lett.* **98**, 124301 (2007).
 - [9] R. D. Deegan, P. J. Petersan, M. Marder, and H. Swinney, *Phys. Rev. Lett.* **88** 014304 (2002).
 - [10] J. Fineberg and M. Marder, *Phys. Rep.* **313**, 1 (1999).
 - [11] A. Livne, E. Bouchbinder, and J. Fineberg, *Phys. Rev. Lett.* **101**, 264301 (2008).
 - [12] V. R. Krishnan, C.-Y. Hui, and R. Long, *Langmuir* **24**, 14245 (2008).
 - [13] A. N. Gent, *Langmuir* **12**, 4492 (1996).
 - [14] T. Baumberger, C. Caroli, D. Martina, *Eur. Phys. J. E* **21**, 81 (2006).
 - [15] R. S. Rivlin, A. G. Thomas, *J. Polymer Sci.* **10**, 291 (1953).
 - [16] K. B. Broberg, *Cracks and fracture* (Academic Press 1999).
 - [17] L. Guo, R. H. Colby, C. P. Lusigan and A. M. Howe, *Macromolecules* **36**, 10009 (2003).
 - [18] O. Ronsin, T. Baumberger and C. Caroli, *Phys. Rev. Lett.* **103**, 138302 (2009).
 - [19] L.R.G. Treloar, *The Physics of Rubber Elasticity* (Oxford University Press, London 1949).

- [20] See `ftp://ftp.insp.jussieu.fr/pub/users/.ronsin/ CrackBranching.htm` for video movies.
- [21] K. E. Daniels, S. Mukhopadhyay, P.J. Houseworth and R. P. Behringer, Phys. Rev. Lett **99**, 124501 (2007).
- [22] E. Bouchbinder, A. Livne, and J. Fineberg, Phys. Rev. Lett. **101**, 264302 (2008).
- [23] M. Shibayama and M. Okamoto, J. Chem. Phys. **115**, 4285 (2001).
- [24] Surface tension could help nucleating cracks at the pinned contact line of the drop, as described for very soft gels in reference [21]. This is not observed here, however.